First-principles study of lattice dynamics of TiO_2 in brookite and cotunnite structures

E. Shojaee,[1] M. Abbasnejad,[1] M. Saeedian,[1] and M. R. Mohammadizadeh[1,2,*]

[1]*Superconductivity Research Laboratory (SRL), Department of Physics, University of Tehran, North Karegar Ave., P.O. Box 14395-547, Tehran, Iran*

[2]*Department of Physics, Brock University, St. Catharines, Ontario, Canada L2S 3A1*

(Received 4 May 2010; revised manuscript received 2 July 2010; published 9 May 2011)

The zone-center phonons and dielectric properties of orthorhombic brookite and cotunnite structures TiO_2 were studied in the framework of density functional perturbative theory. The dielectric properties of brookite and anatase structures are similar. The calculated static dielectric permittivity of brookite is found to be slightly higher than that of anatase, but far lower than that of the rutile structure. This is in contrast with the recent experimental report on brookite flowers. Our study suggests that the static dielectric constant of cotunnite structure is smaller than those of rutile and brookite structures. We obtained the full phonon band structure and elastic properties of these structures. The bulk modulus and Debye temperature of brookite are intermediate between those of the anatase and rutile structures. The obtained value of 301 GPa for the bulk modulus of cotunnite is in good agreement with the stiffness of the material reported experimentally. Because of the similarity in z-direction packing of the TiO_6 tetrahedron between brookite and rutile structures, the elastic constants associated with the z-polarized movement of atoms in brookite are similar to those of the rutile structure. The elastic constants of brookite associated with the movement of the atoms in x-y plane, are similar to the corresponding constants in anatase and rutile structures. This demonstrates the similarity between the packing character of the brookite structure with both anatase and rutile structures. So, the lattice dynamics of brookite is intermediate between those of anatase and rutile polymorphs. The calculated phonon density of states of cotunnite shows that it is stable at ambient pressure.

DOI: 10.1103/PhysRevB.83.174302 PACS number(s): 71.15.Mb, 63.20.D−, 62.20.−x

I. INTRODUCTION

Due to its wide applications in photoactive devices and biomaterials,[1] TiO_2 has been extensively studied. Among its natural polymorphs, rutile has been investigated more than others due to its stability. However, it has been shown that anatase is more efficient in photocatalysis and in solar cell applications.[2–4] Brookite is the least investigated naturally stable form of TiO_2, as it is difficult to synthesize its pure samples unaccompanied by secondary anatase or rutile phases. As methods of fabrication of pure brookite TiO_2 have been developed successfully (see Ref. 5, and references therein), the study of this polymorph of titanium dioxide has received great interest in the past few years. Actually, it has been shown that brookite may exhibit more photocatalytic oxidation activity and photoinduced hydrophilicity than rutile and anatase phases.[6] The static dielectric constant of brookite flowers has been reported to be comparable to that of rutile.[5] This suggests the use of brookite in electronic devices and dielectric materials such as metal-oxide semiconductor transistors.[5]

The other orthorhombic structure of TiO_2, which has gained wide interest, is the cotunnite phase. This structure has been predicted to be as hard as the diamond.[7] Designing ultrahard materials to replace diamond is of both technological and scientific interest. To accomplish this goal, two different aspects have been studied in the literature: (i) investigation of light element compounds such as carbon nitrides[8] and (ii) introducing light elements into the transition metals such as ReB_2[9] in order to increase the bulk modulus. Concerning the latter, both advanced theoretical and experimental methods have been applied. Following this, many theoretical studies have been reported for the structural and electronic properties of cotunnite.[7,10–19]

Raman spectra of natural brookite crystals and the synthesized powders and flowers have been studied recently.[5,20,21] Mo and Ching[22] studied the structural and optical properties of the three naturally grown polymorphs of TiO_2. Due to the lack of experimental data at that time, they were not able to compare their results for brookite with the experiments. Today, we know that their calculated electronic dielectric permittivity is not consistent with the new experimental observations.[5] Gong and Selloni[23] have studied the structures and energetics of ten stoichiometric 1×1 low-index surfaces of brookite phase. Despite all the other polymorphs of TiO_2,[10,24–27] including the non-natural forms, there are few reports on the lattice dynamics of the brookite structure. Posternak *et al.*[28] have studied the Born effective charges of brookite in terms of the Wannier functions and have shown that the crystallographic data in brookite are intermediate between those of the rutile and anatase structures. In a mechanical aspect, using stress-strain analysis, Yao *et al.*[29] have calculated the bulk and shear modulus of brookite. Up to now, there is no experimental report on the elastic stiffness constants of brookite.

The elastic stiffness constants of cotunnite have been investigated by Carvaca *et al.*[11,15] Recently, significantly lower room-pressure bulk modulus compared to a previous experimental report[7] has been obtained.[12,13] Kim *et al.*[10] have calculated the phonon density of states of the cotunnite phase. They concluded that the cotunnite structure is stable above 8 GPa pressures. To our knowledge, there are no reports on the dielectric properties and phonon frequencies of cotunnite.

Therefore, as the interest in brookite and cotunnite phases of TiO_2 is increasing, due to the brookite's photocatalytic and dielectric properties and the cotunnite's hardness, it seems

TABLE I. The optimized lattice parameters and Ti-O bond lengths of the brookite phase.

	Lattice parameters (Å)			
	a	*b*	*c*	Ti-O bond lengths (Å)
This work (LDA)	9.048	5.369	5.057	1.841, 1.890, 1.906, 1.950, 1.984, 2,023
This work (PW91)	9.213	5.468	5.154	1.861, 1.920, 1.933, 2.001, 2.015, 2.078
PBE[a] (Ref. 23)	9.140	5.407	5.176	1.927, 1.929, 1.936, 1.950, 1.978, 1.987
Exp. (Ref. 38)	9.166	5.436	5.135	

[a]Perdew-Burke-Ernzerhof.

necessary to study the lattice dynamics of these polymorphs in more detail.

In the present work, we study the brookite and cotunnite structures of TiO_2 using the density functional theory (DFT) formalism. The rest of the paper is arranged as follows. Section. II presents the computational details. In Sec. III, the electronic properties of brookite and cotunnite are briefly reviewed. In Sec. III A, the lattice dynamics of the structures are presented in the framework of density functional perturbative theory (DFPT). The dielectric properties are considered in Sec. III B. In Sec. III C, the full phonon band structures and the elastic and thermal properties of the orthorhombic phases, such as the full elastic constant tensor and Debye temperature, are reported and discussed.

II. COMPUTATIONAL DETAILS

Total energy and phonon calculations were carried out using the QUANTUM-ESPRESSO package.[30] This package uses pseudopotentials to describe the ion-electron interactions and utilizes a plane-wave basis set to expand the wave functions and charge density. The Perdew-Zunger[31] ultrasoft[32] pseudopotentials were used for titanium and oxygen atoms in the local-density approximation (LDA) and Perdew-Wang[33] ultrasoft pseudopotentials in the generalized-gradient approximation (GGA). In the titanium (oxygen) pseudopotential, $3s, 3p, 4s$, and $3d$ ($2s$ and $2p$) electrons were included in the calculations. The structures were fully optimized, where forces on the ions were less than 0.002 eV/Å and the stresses on the unit-cell faces were less than 2 kbar. Cutoff energies for plane-wave basis set expansions in the wave function and charge density were 44 (45) and 880 (1000) Ry, respectively, in the case of the brookite (cotunnite) structure. The Brillouin zone (BZ) integration for the energy calculation of brookite (cotunnite) was performed with k points in a $2 \times 4 \times 4$ ($6 \times 8 \times 6$) grid with 4 (36) reduced number of k points in the irreducible edge of the first BZ.

The phonon calculations were performed in the framework of DFPT.[34–36] The dynamical matrix (DM) elements associated with the wave vector are found by solving self-consistent coupled equations of the variation of potential and the linear response of electronic density.[34]

In order to obtain the phonon band structure of brookite (cotunnite), the DM was constructed for q vectors in the Monkhorst-Pack $2 \times 2 \times 2$ ($4 \times 4 \times 4$) grid sampling with a shift to include the Gamma point, reduced to 8 (27) q points in the irreducible edge of the first BZ. The interatomic force constants were then obtained by Fourier transformation. The slopes of the linear parts of acoustic branches in phonon band structure lead us to the velocities of the sound propagating in the corresponding directions, and therefore the elastic constants.[37]

TABLE II. The optimized structural parameters of the cotunnite TiO_2 in both the LDA and PW91. The digits in parentheses represent the number of equivalent bonds.

	This work (LDA)	This work (PW91)	Exp. (Ref. 7)
a (Å)	5.181	5.214	5.163
b (Å)	3.043	3.150	2.989
c (Å)	6.069	6.256	5.966
Ti(x)	0.116	0.106	0.110
Ti(y)	0.250	0.250	0.250
Ti(z)	0.244	0.252	0.264
$O_I(x)$	0.426	0.418	0.422
$O_I(y)$	0.250	0.250	0.250
$O_I(z)$	0.359	0.363	0.346
$O_{II}(x)$	0.341	0.347	0.325
$O_{II}(y)$	0.750	0.750	0.750
$O_{II}(z)$	0.024	0.014	0.012
	This work (LDA)	(Ti-O_I): 1.975, 1.984(2), 2.010	(Ti-O_{II}): 2.055, 2.120(2), 2.341(2)
Ti-O bond length (Å)	This work (PW91)	(Ti-O_I): 2.041, 2.054(2), 2.032	(Ti-O_{II}): 2.026, 2.108(2), 2.511(2)
	Ref. 16 (LDA)	1.975, 1.984(2), 2.016,	2.056, 2.127(2), 2.342(2)

TABLE III. The principal-axis values of the Born effective charges of the brookite structure.

Principal values of Born effective charge	Z_1^{*Ti}	Z_2^{*Ti}	Z_3^{*Ti}	$Z_1^{*O_I}$	$Z_2^{*O_I}$	$Z_3^{*O_I}$	$Z_1^{*O_{II}}$	$Z_2^{*O_{II}}$	$Z_3^{*O_{II}}$
This work (LDA)	7.10	6.57	5.10	−5.38	−1.21	−2.83	−5.22	−1.22	−3.16
This work (PW91)	6.72	7.00	4.98	−5.35	−1.22	−2.76	−5.28	−1.20	−3.10

III. RESULTS AND DISCUSSION

The optimized lattice parameters and Ti-O bond lengths of the brookite structure of TiO_2 are presented in Table I. The detailed study on the structure of brookite can be found in Refs. 23, 28, and 39. Using both LDA and PW91, we predict that the brookite structure is a semiconductor with a direct energy gap of 2 eV, in agreement with other theoretical reports.[22,28] It is known that the DFT band gap is underestimated.[40] As the bond lengths are larger in PW91, one may expect to predict a smaller value for the band gap, compared to the LDA result. However, it has been shown that the TiO_2 polymorphs do not follow the simple bond-length–band-gap correction.[41] This suggests that the decrease of the band gap is due to increased bond lengths. Among the experimental studies, Zallen and Moret[20] show that the natural brookite crystal has an indirect electronic band gap of 1.9 eV, in contrast with the band-structure calculations.[22,28,42] Di Paola and Cufalo[43] have obtained the value of 3.26 eV for the band gap of brookite powder by diffuse reflectance measurements. Recently, Hu and Li[5] have reported the fabrication of high-quality brookite flowers via a facile solution chemistry technique. These pure phase brookite flowers have shown a direct transition with a band-gap energy of 3.4 eV.

Concerning the cotunnite structure, the optimized structural parameters including lattice and the internal parameters and the Ti-O bond lengths of cotunnite in the LDA and PW91 are presented in Table II . Detailed studies on the cotunnite structure are presented in Refs. 11, 14–17, and 19. Although LDA usually underestimates the lattice parameters and PW91 yields results in better agreement with the experiment, the ones computed with the LDA and PW91 are overestimated. The reason for this is that the experimental lattice parameters were determined *in situ* at pressure 61 GPa, whereas the former is a minimum-energy calculation at equilibrium conditions. The electronic band structure and density-of-states calculations indicate a band gap of 1.5 (1.6) eV in the LDA (PW91) which is comparable with the other reports.[11,16,19] There is no experimental report on the cotunnite band-gap energy, but similar to the previous computational and experimental results reported for the other phases of TiO_2 such as rutile and anatase,[44–46] we expect the band gap is underestimated.

A. Lattice dynamics

1. *Brookite structure*

The calculated principal-axis values of Born effective charges for Ti, O_I, and O_{II} atoms in the both LDA and PW91 are presented in Table III . The Born effective charge tensors of Ti atoms are intermediate between those of anatase and rutile, while the Born effective charge tensors for two types of O atoms are anatase and rutilelike.[27,28]

By means of factor analysis,[47] in the space group for the brookite phase ($Pbca$), the irreducible representations of optical vibrations are

$$\Gamma_{\text{opt}} = 9A_{1g} + 9B_{1g} + 9B_{2g} + 9B_{3g} + 9A_{1u} + 8B_{1u} + 8B_{2u} + 8B_{3u},$$

where A_{1g}, B_{1g}, B_{2g}, and B_{3g} are Raman active, B_{1u}, B_{2u}, and B_{3u} are IR active, and A_{1u} modes are silent. The calculated Raman and IR modes in the LDA and PW91 are listed in Tables IV and V, respectively. The experimental observations[5,21] have detected 15 and 18 out of 36 Raman modes of the brookite structure for the flowers and the synthesized powders, respectively. In the case of IR spectrum, Tompsett and Bowmaker[21] have reported the bands in the 3300–3400 cm^{-1} region, which they believe arise from protons associated with the oxygen ions adjacent to a trivalent metallic ion substituting at a tetravalent titanium site (Fe^{3+} for Ti^{4+}). Hu and Li[5] have observed four distinct vibrations at 420, 488, 564, and 710 cm^{-1}. They do not detect vibrations above 1000 cm^{-1}.

The B_u modes of brookite should, in general, exhibit LO-TO splitting. As the structure is orthorhombic, these splittings occur in the three Cartesian directions. The B_{1u} modes that do not preserve the σ_{xy} symmetry of the space group are modes in which the movement of the Ti atoms in the unit cell in the z direction is collective, and the sum of the projection of the Ti atomic displacements on the x (and y) axis is zero. The same happens for the two types of O atoms, separately.

TABLE IV. The Raman-active modes of the brookite phase in cm^{-1}.

	This work (LDA)	This work (PW91)	Exp. (Ref. 5)	Exp. (Ref. 21)
A_{1g}	125, 161, 182, 231, 346, 428, 498, 573, 656	120, 148, 186, 240, 308, 391, 477, 530, 622	155, 194, 247 412, 636	128, 153, 195, 247, 412, 636
B_{1g}	176, 233, 334, 365, 396, 471, 496, 594, 780	153, 238, 319, 353, 380, 446, 463, 554, 736,	213, 322, 501	135, 214, 322, 502
B_{2g}	162, 212, 297, 322, 382, 463, 516, 631, 839	165, 209, 279, 318, 366, 432, 497, 596, 798	366, 395, 460, 583	366, 396, 461, 585
B_{3g}	142, 205, 288, 322, 444, 443, 515, 545, 828	122, 210, 283, 298, 401, 429, 494, 511, 787	172, 287, 545	172, 288, 454, 545

TABLE V. The IR-active modes of the brookite phase in cm^{-1}.

	This work (LDA)	This work (PW91)	Exp. (Ref. 5)
A_{1u}	139, 243, 290, 305, 348, 394, 511, 581, 659	115, 242, 271, 284, 342, 366, 472, 542, 622	
B_{1u} (TO)	208, 233, 295, 322, 403, 481, 561, 879	189, 218, 284, 314, 367, 467, 517, 838	
(LO)	208, 792, 295, 312, 385, 442, 515, 892	214, 761, 280, 296, 357, 428, 479, 849	
B_{2u} (TO)	154, 180, 244, 379, 432, 502, 612, 682	149, 164, 230, 363, 400, 469, 579, 648	420, 488, 564, 710
(LO)	156, 180, 365, 379, 856, 489, 563, 681	149, 167, 813, 372, 346, 460, 530, 647	
B_{3u} (TO)	191, 240, 333, 362, 423, 475, 533, 851	185, 209, 313, 340, 397, 445, 510, 811	
(LO)	192, 882, 311, 357, 384, 460, 510, 829	188, 791, 304, 340, 367, 438, 491, 842	

This collective movement of the atoms may contribute to the static dielectric constant of the crystal, and as a consequence, LO-TO splitting occurs. That is what happens in the B_{2u} (B_{3u}) modes, in which the collective movement of the same type of atoms in the y (x) direction, breaks the σ_{xz} (σ_{yz}) symmetry and exhibits LO-TO splitting. In order to obtain the longitudinal optical modes at $q = 0$, a nonanalytical direction-dependent term (which contains the values of the Cartesian components of the dielectric tensor and the Born effective charges) was added to the dynamical matrix elements at $q = 0$ [see Eq. (18) of Ref. 34]. The giant LO-TO splitting in the B_{1u} modes is related to the mode with frequency 233(218) cm^{-1}, which couples with the electric field and generates an LO mode equal to 792(761) cm^{-1} (the figures in parentheses are the PW91 values). In the case of B_{2u} modes, there are two major splittings related to the frequencies 244(230) cm^{-1} and 432(400) cm^{-1}, which generate 365(346) cm^{-1} and 856(813) cm^{-1} modes. Among the B_{3u} modes, the modes with frequencies 240(209) cm^{-1} and 423(397) cm^{-1} are responsible for the large splittings and generate 384(367) cm^{-1} and 882(791) cm^{-1} modes. In order to refine the coupling between the TO and LO modes, we have obtained an estimation of the LO modes associated with the TO's, using the method in Ref. 36. For example, the LO mode obtained by the above equation for the 240(209) cm^{-1} B_{3u} (TO) mode is 549(588) cm^{-1} and for the 423(397) cm^{-1} B_{3u} (TO) mode it is 541(489) cm^{-1}. This method suggests that the 882(791) cm^{-1} B_{3u} (LO) mode should be paired to the 240(209) cm^{-1} B_{3u} (TO) mode, which gives a large splitting. As presented in Tables IV and V, the Raman- and IR-active modes of the brookite phase using PW91 are less than the LDA values (as in the case of the anatase and rutile structures[27]). Consequently, the calculated static dielectric tensor within the PW91 is larger than the LDA one (Sec. III B).

2. *Cotunnite structure*

The principal values of effective charge tensor elements of cotunnite (obtained by diagonalization of the Born effective charge tensor) were presented in Table VI in both the LDA and PW91. The values for the PW91 are larger than the LDA, which is expected due to the larger bond lengths of PW91. The principal values of effective charges are close to the charges in a pure ionic-bond picture, which are +4 for Ti and −2 for O atoms, whereas the effective charges are larger in the rutile, anatase, and brookite structures.[24,26,27] This shows the greater ionicity of the cotunnite structure compared to the other polymorphs. This character shows its effect when calculating the static dielectric constants of cotunnite.

According to the group theory analysis,[47] the irreducible representations of the optical vibrations are as follows:

$$\Gamma_{\text{opt}} = 6A_{1g} + 3B_{1g} + 6B_{2g} + 3B_{3g} + 3A_{1u} + 5B_{1u} + 2B_{2u} + 5B_{3u}.$$

Only the 12 infrared-active modes with B_u symmetrical species contribute to the lattice dielectric tensor (Sec. III B of the present paper). For example, in the B_{1u} (B_{3u}) modes, the equivalent atomic displacements in the z (x) direction are collective; so, the B_{1u} modes are responsible for the z(x)-component of the dielectric tensor. The zone-center phonon frequencies of the cotunnite structure calculated in the present work in both the LDA and PW91 are presented in Table VII. The 387(355) and 490(450) cm^{-1} B_{1u}, the 338(305) cm^{-1} B_{2u}, and the 240(220), 430(378), and 459(406) cm^{-1} B_{3u} modes in the LDA(PW91) have large oscillator strengths[36] among the IR-active modes. Generally, the IR-active modes exhibit LO-TO splitting. Similar to the brookite structure, splitting may occur in the three Cartesian directions. Based upon the construction of the overlap matrices and the oscillator strengths,[36] there is no significant splitting between the longitudinal and transverse optical modes as in the case of the rutile and anatase structures[24,26,27] and the brookite phase as presented in the previous section. This is consistent with the small magnitude of the Born effective charges of atoms obtained for the cotunnite structure, compared to those of the rutile and anatase phases. To our knowledge, there is no computational or experimental report on this issue on cotunnite TiO_2.

TABLE VI. The principal values of the Born effective charge tensor elements of the cotunnite TiO_2.

Principal values of Born effective charge	Z_1^{*Ti}	Z_2^{*Ti}	Z_3^{*Ti}	$Z_1^{*O_I}$	$Z_2^{*O_I}$	$Z_3^{*O_I}$	$Z_1^{*O_{II}}$	$Z_2^{*O_{II}}$	$Z_3^{*O_{II}}$
This work (LDA)	4.74	5.03	4.83	−2.11	−2.84	−2.12	−2.76	−2.21	−2.79
This work (PW91)	5.22	4.81	5.06	−2.31	−2.86	−2.22	−2.81	−2.20	−2.91

TABLE VII. The silent, IR, and Raman-active modes of cotunnite TiO_2 in cm^{-1}.

Γ modes		Wave number (cm^{-1}) This work (LDA)	This work (PW91)
A_u (silent)		150, 335, 511	115, 327, 447
B_{1u}	TO	191, 387, 491, 658, 666	107, 355, 450, 592, 643
	LO	233, 416, 591, 661, 755	159, 378, 567, 626, 689
B_{2u}	TO	338, 580	305, 521
	LO	505, 687	631, 494
B_{3u}	TO	240, 430, 459, 566, 717	220, 378, 406, 533, 679
	LO	295, 449, 665, 556, 720	254, 396, 649, 527, 679
A_g		212, 329, 393, 473, 625, 687	192, 299, 369, 450, 574, 646
B_{1g}		242, 404, 647	206, 400, 593
B_{2g}		342, 427, 476, 583, 595, 710	292, 414, 443, 543, 578, 649
B_{3g}		227, 436, 646	198, 438, 574

B. Dielectric properties

1. *Brookite structure*

In order to calculate the static dielectric constant in the brookite structure, the ionic contribution must be added to the electronic part. The ionic part has been calculated by the factorized form.[48] The factorized form has been used by Gonzalez *et al*. in the case of anatase, which fits the experimental measurements of the reflectivity very well.[49] The factorized form is more appropriate than the oscillator form[36] for highly ionic crystals, which have large TO-LO splitting.[49] The results of the present work and the experimental observations are listed in Table VIII. The PW91 values are larger (especially in the x direction), because the frequency of modes is lower in PW91 (compared to the LDA results). As there are no sufficient experimental data on IR spectra of the brookite phase, there is no way to find out which one of the LDA or PW91 results predicts the IR spectra in better agreement with the experiment. In the anatase and rutile phases, the zone-center phonons in PW91 are smaller than the LDA and less comparable to the experiments.[27] However, the calculated value for static dielectric permittivity is different from the experimental report by Hu and Li,[5] who reported the permittivity for the brookite flowers is much higher than that of the anatase structure, but is slightly lower than that of the rutile structure.[5] The LO-TO splitting for brookite is very similar to the anatase result,[26,27] while the giant splitting in the rutile structure is a sign of the great dielectric permittivity.[24] So, we believe that the dielectric permittivity for brookite should be closer to the anatase one rather than to that of the rutile structure. The procedure which the authors in Ref. 5 have used to prepare the brookite flowers for complex ac impedance measurements, consists of pressing and heating up to 500°C, which is near the structural phase-transition temperature of brookite-rutile.[50] However, they claim that the sample maintained the pure brookite phase without microstructural collapse.[5] We should also mention there are usually discrepancies among the experimental values of the static dielectric permittivity, similar to the case of rutile structure.[51]

2. *Cotunnite structure*

The calculated electronic (high-frequency) dielectric constant tensor of the cotunnite structure in both the LDA and PW91 are reported in Table VIII. There are no corresponding experimental values available yet. The cotunnite electronic dielectric constants are larger than those of rutile, anatase, and

TABLE VIII. The electronic ($\varepsilon_{ij}^{\infty}$) and static ($\varepsilon_{ij}^{0}$) dielectric permittivity tensors of the brookite, cotunnite, anatase, and rutile phases.

		$\varepsilon_{ij}^{\infty}$			ε_{ij}^{0}		
		xx	yy	zz	xx	yy	zz
brookite	This work (LDA)	7.49	6.96	6.86	58.2	50.2	50
	This work (PW91)	7.51	6.75	6.78	86.7	55.2	64.1
	Exp. (Ref. 5)					93	
cotunnite	This work (LDA)	9.56	9.23	9.46	33.3	28.9	30.6
	This work (PW91)	9.89	9.38	9.27	36.1	36.1	47.3
anatase	Ref. 26 (LDA)	7.07	7.07	6.21	45.9	45.9	24.4
	Ref. 27 (PW91)	7.10	7.10	6.29	48.7	48.7	33.2
	Exp. (Ref. 49)	5.82	5.82	5.41	45.1	45.1	22.7
rutile	Ref. 24 (LDA)	7.54	7.54	8.67	117.5	117.5	165.4
	Ref. 27 (PW91)	7.39	7.39	8.40	265.2	265.2	373.3
	Exp. (Ref. 51)	6.84	6.84	8.43	86	86	170

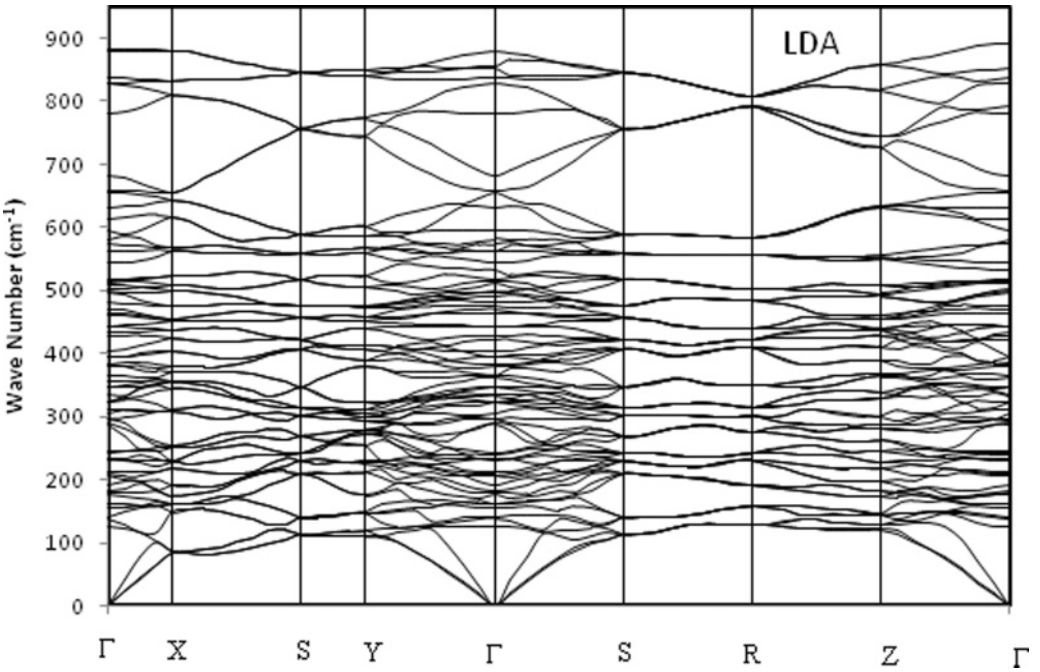

FIG. 1. Phonon band structure of the brookite TiO_2 within the LDA.

brookite (Table VIII), which show larger ionic polarizability than those structures. Based upon the factorized form of the static dielectric constant described by Kurosawa,[48] the elements of the static dielectric tensor of the cotunnite structure have been calculated. It can be seen that the static dielectric constants of the cotunnite structure are close to those of the anatase structure. The modes corresponding to the static dielectric constants of the cotunnite structure are the B_u ones. As presented in the Table VIII, the softening of the zone-center phonons in the PW91 (compared to the LDA), leads to almost larger static dielectric constants, which may be fictitious due to the underestimation of the modes. The magnitude of the static dielectric constants in the cotunnite structure is smaller than those of the rutile and anatase phases.[24,26]

C. Elastic and thermal properties

1. Brookite structure

The full phonon band structure of brookite in the LDA is presented in Fig. 1. The common path, including high symmetry points for orthorhombic structures, is not suitable for demonstrating the LO-TO splitting, thus the splittings are not presented in the phonon band structure. (The LO-TO splittings are discussed in detail in Sec. III A.) The phonon density of states in the LDA and PW91 (Fig. 2) show that the PW91 leads the phonon band structure to shift down to lower frequencies, so we did not find it necessary to present the full phonon band structure in PW91. To check whether the number of interatomic force constants is sufficient to obtain

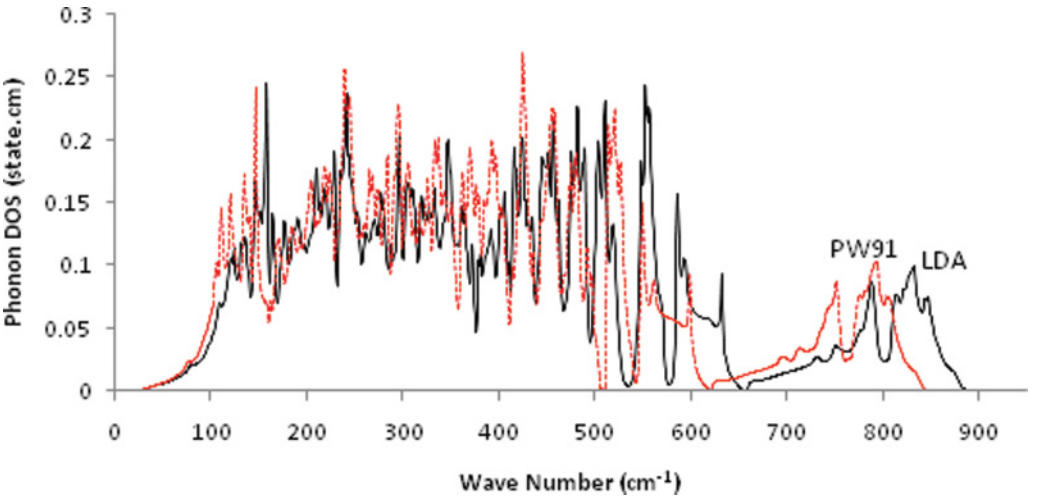

FIG. 2. (Color online) Phonon density of states of the brookite TiO_2. The bold line represents the LDA and the dashed line represents the GGA (PW91).

TABLE IX. The elastic constant tensor (C_{ij}), bulk (B_{VRH}) and shear (G_{VRH}) modulus of the brookite phase in GPa and Debye temperature (Θ_{D}) in K.

	C_{11}	C_{12}	C_{13}	C_{22}	C_{23}	C_{33}	C_{44}	C_{55}	C_{66}	B_{VRH}	G_{VRH}	θ_{D}
This work (LDA)	317	192	281	304	160	355	94	104	103	245	72	608
This work (PW91)	308	164	240	281	142	339	91	106	87	221	77	636
Ref. 29 (LDA)	315	191	184	351	164	310	113	106	107	228	92	
Ref. 29 (GGA)	285	156	159	302	141	289	102	95	88	199	84	

the phonon bands, we have calculated the dynamical matrix of several general points in the first BZ, directly. The rms difference between the frequencies, which were obtained by the direct or extrapolation methods, was less than 3 cm^{-1}, which seems reasonable. Similar to the case of anatase and rutile structures,[27] the PW91 shifts the phonon frequencies to lower amounts, which shows that the three natural polymorphs of TiO_2 have positive Gruneissen parameters. The pseudogap in the phonon density of states of brookite, which is located in the high-frequency region, is more similar to that of the anatase structure. It shows that the polarity character of brookite is similar to that of the anatase structure.[27] This feature has been demonstrated by calculation of the static permittivity of brookite and comparing it with the other polymorphs (Sec. III B).

The elastic constants of the brookite, anatase, and rutile structures (Tables IX and X) are calculated by linear fit to the acoustic branches. In the case of the brookite phase, the elastic constants are in good agreement with the work performed by the stress-strain method,[29] except in C_{13}, for which the results are different. The greater value of C_{33} is reasonable, since the packing of the tetrahedron in the brookite is very similar to that of the rutile structure, and the stiffness in the z direction of brookite should not be much different from the rutile phase value. In addition, the elastic constants corresponding to the z-polarized movement of the atoms in the brookite phase, i.e., C_{44} and C_{55}, are comparable to the C_{44} of the rutile phase, which seems acceptable according to the similar packing pattern in the z direction between the brookite and rutile structures. On the other hand, as the packing pattern of the TiO_6 octahedron in the brookite unit cell is similar to both the anatase and rutile structures in the x-y plane, the elastic constants associated to the in-plane atomic movements C_{11} and C_{22} are comparable to the corresponding constants of anatase and rutile, i.e., C_{11}.

Calculated bulk modulus (B_{VRH}), shear modulus (G_{VRH})–based on Voigt-Reuss-Hill approach [53–55]–and Debye temperature (Θ_D) of brookite TiO_2 are presented in Table IX. These values are between those corresponding values of the anatase and rutile structures. It suggests that the hardness of the brookite phase is also an intermediate value between those of the anatase and rutile phases.[27]

2. *Cotunnite structure*

In order to study the structural stability of the cotunnite phase, the full phonon band structure in the LDA was obtained (Fig. 3). There are no modes with imaginary frequency, which confirms the dynamical stability of the structure. As for the brookite, the reliability of the chosen number of interatomic force constants to obtain the phonon bands has been verified. The PW91 phonon density of states has a shift to the low frequencies compared to the LDA (Fig. 4), similar to the natural phases of TiO_2.[27] As the phonon density of states for cotunnite in both the LDA and PW91 are in the positive region, we believe the cotunnite phase can be stable at ambient pressure. This finding is in agreement with the experiment,[7] which argued that the cotunnite TiO_2 can be preserved in rapid decompression from 60 GPa to ambient pressure at 77 K. However, Kim *et al*. with the DFT-GGA calculations[10] claim that the cotunnite phase is not stable at pressures below 8 GPa, which is not in agreement with our results. They have calculated the phonon density of states based on the *ab initio* force-constant method. The Ti-O bond lengths of rutile obtained in their work were overestimated compared to the other results.[23,27] This impacted the reduction of the binding energy and consequently, the frequency modes. It can be the origin of the difference between their results and ours. As the LDA tends to phonon frequencies in better agreement with the experiments in the case of other TiO_2 polymorphs,[27] we expect the LDA calculation to be more appropriate to verify whether the structure is stable or not at ambient pressure. Unlike the natural structures, including brookite, there is no pseudogap in the phonon density of states of cotunnite. This phenomenon may be related to the smaller values of Born effective charges in the cotunnite phase (Table VI) compared to the natural structures.

TABLE X. The elastic constant tensors (C_{ij}) of the anatase and rutile phases in GPa.

	Anatase						Rutile					
	C_{11}	C_{12}	C_{13}	C_{33}	C_{44}	C_{66}	C_{11}	C_{12}	C_{13}	C_{33}	C_{44}	C_{66}
LDA (Ref. 27)	399	156	152	203	34	60	303	222	205	561	113	251
PW91 (Ref. 27)	333	143	140	198	39	57	269	189	166	506	105	217
Exp. (Ref. 52)							271	177	149	484	124	194

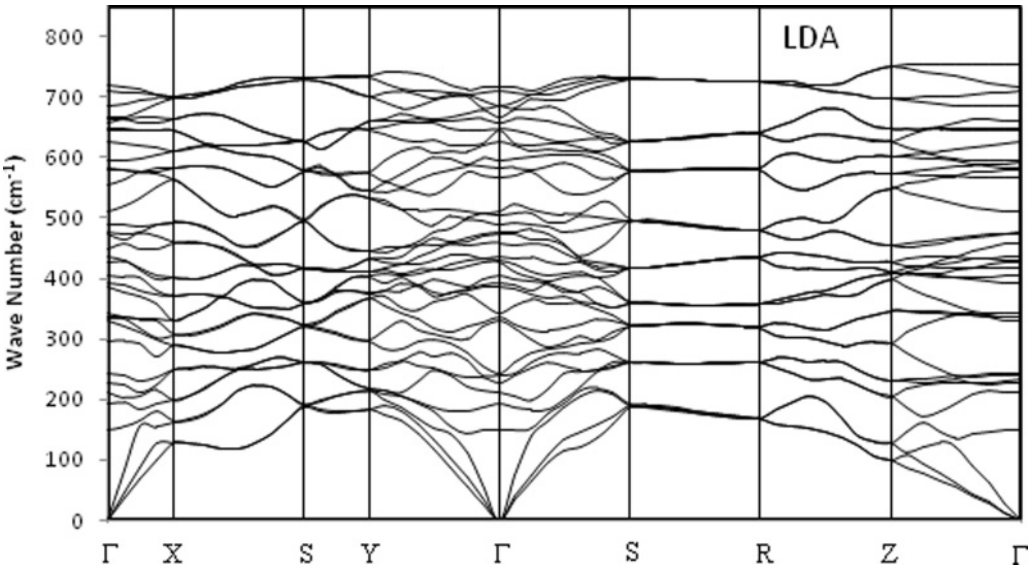

FIG. 3. Phonon band structure of the cotunnite TiO_2 within the LDA.

The elastic constants calculated in the present work in both the LDA and PW91 are presented in Table XI and compared with the other results obtained by the stress-strain method.[11,15,18] Koci *et al.*[17] have studied the C_{44} elastic constant of cotunnite as a function of pressure up to 70 GPa. Their results at zero pressure are very large compared to ours and those of other reports.[15,18] The calculated bulk modulus, shear modulus, and Debye temperature of the cotunnite TiO_2 are also presented in Table XI. It can be seen that the PW91 values for the stiffness of the crystal are dramatically smaller than those of the LDA. According to our data, cotunnite is the hardest phase among the polymorphs of TiO_2. The inconsistency between our results and those of Refs. 11 and 15 is more considerable in the cases of C_{11}, C_{22}, and C_{33}, where our values are much smaller. These three constants play an important role in calculating the bulk modulus using VRH approximation.[53–55] By comparing the values of the calculated bulk modulus in the present work and those of the other works, we can choose the more reliable results. Our calculated bulk modulus in the LDA is in better agreement with the latest experimental reports on the cotunnite structure,[12,13] as presented in Table XI. However, there is a large difference between our reported bulk modulus and those obtained by Dubrovinsky *et al.*[7] The first pressure derivative of bulk modulus $\left(B_0'\right)$ obtained from their experimental data is 1.35, whereas it should be close to 4.0 in the stiff materials.[56] In addition, the Birch-Murnaghan formulation itself is valid only where $\left(B_0'\right)$ is sufficiently close to 4.0.[57] The bulk modulus obtained by the elastic constants of the works by Caravaca *et al.*[11,15] in the LDA is far from the experimental results. So, it seems that the C_{11}, C_{22}, and C_{33} reported in this work are considerably relevant. All the reported GGA values (including ours) for the bulk modulus are far from the experimental observations.

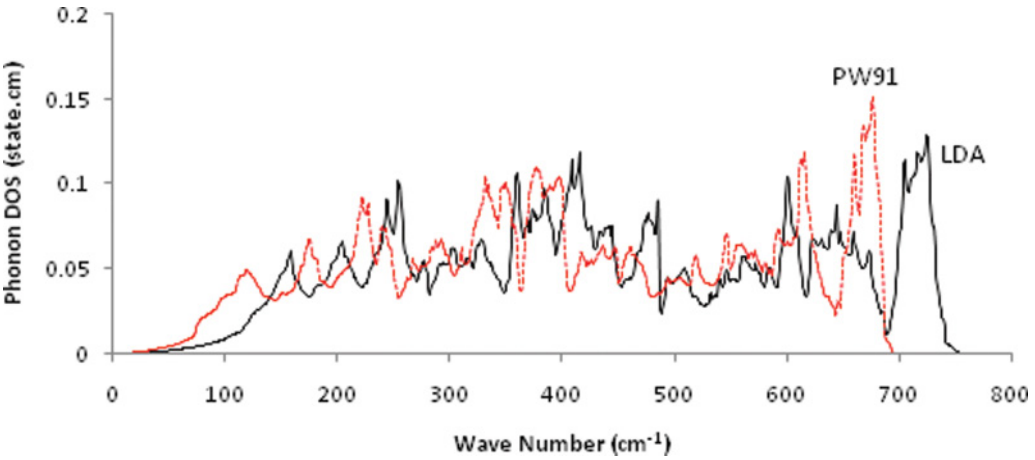

FIG. 4. (Color online) Phonon density of states of the cotunnite TiO_2. The bold line represents the LDA and the dashed line represents the GGA (PW91).

TABLE XI. The elastic constant tensors (C_{ij}), bulk (B_{VRH}), and shear (G_{VRH}) modulus of the cotunnite phase in GPa and Debye temperature (Θ_{D}) in K.

	C_{11}	C_{12}	C_{13}	C_{22}	C_{23}	C_{33}	C_{44}	C_{55}	C_{66}	B_{VRH}	G_{VRH}	θ_{D}
This work (LDA)	555	234	237	408	196	450	89	109	159	301	119	748
This work (PW91)	474	190	202	258	90	224	62	13	127	187	55	520
Refs. 11 and 15 (LDA)	688	258	240	510	253	649	129	133	204	370	162	904
Ref. 15 (GGA)	619	218	178	350	82	282	52	43	219	221	96	
Ref. 18 (GGA)	478	165	191	291	85	279	58	38	129	200	77	

IV. CONCLUSIONS

The electronic and dynamical properties of the brookite and cotunnite TiO_2–the least-studied stable form of TiO_2 and the hardest known oxide, respectively—were studied by the first-principles calculations based on the DFT and DFPT. As the crystallographic data in brookite are intermediate between those of anatase and rutile, it is expected that the other properties be the same. The Born effective charges and dielectric permittivity tensor for both the brookite and cotunnite structures have been obtained and compared to those of the anatase and rutile phases. The calculated Born effective charges of the cotunnite phase are close to the charges in a pure ionic-bond picture, in contrast to the other polymorphs. It is shown that the static dielectric permittivity of brookite is slightly larger than that of anatase, but is much smaller than that of rutile. The cotunnite static dielectric permittivity is close to that of anatase. The zone-center phonon frequencies, including Raman- and IR-active modes are studied and compared with the available experimental reports. Due to difficulties in synthesizing pure brookite, there are no complete experimental reports on the properties of this polymorph, and there are no experimental results on the dynamical properties of the cotunnite structure, to our knowledge. The full phonon band structures for the polymorphs are reported and the elastic constants are obtained by a linear fit to the acoustic branches of the phonon band structure in symmetry directions. The phonon density of states of the cotunnite obtained in both the LDA and PW91 show that this structure is stable at ambient pressure.

In the brookite structure, packing of the TiO_6 octahedron in [100] and [010] directions is like both the anatase and rutile structures, while in the [001] direction it is similar to the rutile structure. As a consequence, the elastic constants corresponding to the z-polarized movement of the atoms in the brookite phase are similar to those of the rutile phase, and the constants related to the x-y plane-polarized movement are similar to those of both anatase and rutile. Thus, the brookite structure is also an intermediate phase between the anatase and rutile structures, in respect to elastic properties. The values of the isotropic bulk and shear modulus, and the Debye temperature of the brookite phase were also obtained between the anatase and rutile amounts. In the case of the cotunnite structure, the calculated LDA bulk modulus is in good agreement with the experiment, larger than those of the other polymorphs of TiO_2. Therefore, the cotunnite structure is the hardest among the TiO_2 polymorphs, and a candidate for coating prospects.

ACKNOWLEDGMENTS

Partial financial support by the research council of the University of Tehran is acknowledged. The technical support of the Computational Nanotechnology Supercomputing Center at the Institute for Research in the Fundamental Sciences (IPM), S. K. Bose, M. F. Miri, S. M. V. Allaei, S. Mohammadi, and A. Ashrafi are also acknowledged. One of the authors (M.R.M.) would like to thank F. Razavi for his support during his sabbatical at Brock University.

*Present address: Dept. of Physics, Brock University, St. Catharines, ON, Canada L2S 3A1.; zadeh@ut.ac.ir, rmohammadizadeh@brocku.ca

[1] U. Diebold, Surf. Sci. Rep. **48**, 53 (2003).
[2] J. Augustynski, Electrochim. Acta **38**, 43 (1993).
[3] A. L. Linsebigler, G. Lu, and J. T. Yates Jr., Chem. Rev. (Washington D.C.) **95**, 735 (1995).
[4] B. O'Regan and M. Grätzel, Nature (London) **353**, 737 (1991).
[5] W. Hu and L. Li, Cryst. Growth Des. **9**, 3676 (2009).
[6] T. Shibata, H. Irie, M. Ohmori, A. Nakajima, T. Watanabe, and K. Hashimoto, PhysChemChemPhys. **6**, 1359 (2004).
[7] L. S. Dubrovinsky, N. A. Dubrovinskaia, V. Swamy, J. Muscat, N. M. Harrison, R. Ahuja, B. Holm, and B. Johansson, Nature (London) **410**, 653 (2001); R. Ahuja and L. S. Dubrovinsky, J. Phys. Condens. Matter **14**, 10995 (2002); N. A. Dubrovinskaia, L. S. Dubrovinsky, V. Swamy, and R. Ahuja, High Press. Res. **22**, 391 (2002); R. Ahuja and L. S. Dubrovinsky, *ibid.* **22**, 429 (2002).
[8] D. M. Teter and R. J. Hemley, Science **53**, 271 (1996).
[9] H. Y. Chung, M. B. Weinberger, J. B. Levine, A. Kavner, J. M. Yang, S. H. Tolbert, and R. B. Kaner, Science **316**, 436 (2007).
[10] D. Y. Kim, J. S. de Almeida, L. Koci, and R. Ahuja, Appl. Phys. Lett. **90**, 171903 (2007).
[11] M. A. Caravaca, R. A. Casali, and J. C. Mino, Phys. Status Solidi B **246**, 599 (2009).
[12] Y. Al-Khatatbeh, K. K. M. Lee, and B. Kiefer, Phys. Rev. B **79**, 134114 (2009).
[13] D. Nishio-Hamane, A. Shimizu, R. Nakahira, K. Niwa, A. Sano-Furukawa, T. Okada, T. Yagi, and T. Kikegawa, Phys. Chem. Minerals **37**, 129 (2010).

[14]J. Muscat, V. Swamy, and N. M. Harrison, Phys. Rev. B **65**, 224112 (2002).
[15]M. A. Caravaca, J. C. Mino, V. J. Perez, R. A. Casali, and C. A. Ponce, J. Phys.: Condens. Matter **21**, 015501 (2009).
[16]M. Kuo, C. Chen, C. Hua, H. Yang, and P. Shen, J. Phys. Chem. B **109**, 8693 (2005).
[17]L. Koci, D. Y. Kim, J. S. de Almeida, M. Mattesini, E. Isaev, and R. Ahuja, J. Phys.: Condens. Matter **20**, 345218 (2008).
[18]X. Wu, E. Holbig, and G. Steinle-Neumann, J. Phys.: Condens. Matter **22**, 295501 (2010).
[19]J. Z. Zhao, G. T. Wang, and Y. C. Liang, Chin. Phys. Lett. **25**, 4356 (2008).
[20]R. Zallen and M. P. Moret, Solid State Commun. **137**, 154 (2006).
[21]G. A. Tompset and G. A. Bowmaker, J. Raman Spectrosc., **26**, 57 (1995).
[22]Shang-Di Mo and W. Y. Ching, Phys. Rev. B **51**, 13023 (1995).
[23]X. Q. Gong and A. Selloni, Phys. Rev. B **76**, 235307 (2007).
[24]C. Lee and X. Gonze, Phys. Rev. B **49**, 14730 (1994); C. Lee, P. Ghosez, and X. Gonze, *ibid*. **50**, 13379 (1994).
[25]R. Sikora, J. Phys. Chem. Solids **66**, 1069 (2005).
[26]M. Mikami, S. Nakamura, O. Kitao, and H. Arakawa, Phys. Rev. B **66**, 155213 (2002).
[27]E. Shojaee and M. R. Mohammadizadeh, J. Phys.: Condens. Matter **22**, 015401 (2010).
[28]M. Posternak, A. Baldereschi, E. J. Walter, and H. Krakauer, Phys. Rev. B **74**, 125113 (2006).
[29]H. Yao, L. Ouyang, and W. Y. Ching, J. Am. Ceram. Soc. **90**, 3194 (2007).
[30]P. Giannozzi, S. Baroni, N. Bonini, M. Calandra, R. Car, C. Cavazzoni, D. Ceresoli, G. L. Chiarotti, M. Cococcioni, I. Dabo, A. Dal Corso, S. de Gironcoli, S. Fabris, G. Fratesi, R. Gebauer, U. Gerstmann, C. Gougoussis, A. Kokalj, M. Lazzeri, L. Martin-Samos, N. Marzari, F. Mauri, R. Mazzarello, S. Paolini, A. Pasquarello, L. Paulatto, C. Sbraccia, S. Scandolo, G. Sclauzero, A. P. Seitsonen, A. Smogunov, P. Umari, and R. M. Wentzcovitch, J. Phys.: Condens. Matter **21**, 395502 (2009).
[31]D. M. Ceperley and B. J. Alder, Phys. Rev. Lett. **45**, 566 (1980); J. P. Perdew and A. Zunger, Phys. Rev. B **23**, 5048 (1981).
[32]D. Vanderbilt, Phys. Rev. B **41**, 7892 (1990).
[33]J. P. Perdew, in *Electronic Structure of Solids '91*, edited by P. Ziesche and H. Eschrig (Akademie Verlag, Berlin, 1991), p. 11.
[34]P. Giannozzi, S. de Gironcoli, P. Pavone, and S. Baroni, Phys. Rev. B **43**, 7231 (1991).
[35]S. Baroni, S. de Gironcoli, A. Dal Corso, and P. Giannozzi, Rev. Mod. Phys. **73**, 515 (2001).
[36]X. Gonze and C. Lee, Phys. Rev. B **55**, 10355 (1997).
[37]B. Auld, *Acoustic Fields and Waves in Solids* (Wiley, New York, 1973).
[38]R. W. G. Wyckoff, *Crystal Structures* (Interscience, New York, 1963).
[39]G. Cangiani, A. Baldereschi, M. Posternak, and H. Krakauer, Phys. Rev. B **69**, 121101(R) (2004).
[40]R. M. Martin, *Electronic Structure* (Cambridge University Press, Cambridge, 2004); H. Akbarzadeh and M. R. Mohammadizadeh, Comp. Mater. Sci. **8**, 335 (1997).
[41]Ming-Yu Kuo, Cheng-Lung Chen, Chih-Yu Hua, Hsiao-Ching Yang, and Pouyan Shen, J. Phys. Chem. B, **109**, 8693 (2005).
[42]M. Gratzel and F. P. Rotzinger, Chem. Phys. Lett. **118**, 474 (1985).
[43]A. Di Paola and G. Cufalo, Colloids Surf. A **317**, 366 (2008).
[44]J. Pascual, J. Camassel, and H. Mathieu, Phys. Rev. B **18**, 5606 (1978).
[45]H. Tang, F. Levy, H. Berger, and P. E. Schmid, Phys. Rev. B **52**, 7771 (1995).
[46]M. Mikami, S. Nakamura, O. Kitao, H. Arakawa, and X. Gonze, Jpn. J. Appl. Phys., Part 1 **39**, L847 (2000).
[47]W. G. Fateley, F. R. Dollish, N. McDevitt, and F. F. Bentley, *Infrared and Raman Selection Rules for Molecular and Lattice Vibrations: The Correlation Method* (Wiley, New York, 1972).
[48]T. Kurosawa, J. Phys. Soc. Jpn. **16**, 1298 (1961).
[49]R. J. Gonzalez, R. Zallen, and H. Berger, Phys. Rev. B **55**, 7014 (1997).
[50]J. Li and T. Ishigaki, Acta Materialia **52**, 5143 (2004).
[51]G. A. Samara and P. S. Peercy, Phys. Rev. B **7**, 1131 (1973); R. A. Parker, Phys. Rev. **124**, 1719 (1961); J. G. Traylor, H. G. Smith, R. M. Nicklow, and M. K. Wilkinson, Phys. Rev. B **3**, 3457 (1971).
[52]I. J. Fritz, J. Phys. Chem. Solids **35**, 817 (1974); M. H. Manghnani, E. S. Fisher, and W. S. Brower Jr., J. Phys. Chem. Solids **33**, 2149 (1972).
[53]A. Reuss and Z. Angew, Math. Mech. **9**, 49 (1929).
[54]W. Voigt, Wied. Ann. **38**, 573 (1889).
[55]R. Hill, Proc. Phys. Soc., London, Sect. A **65**, 349 (1952).
[56]J. P. Poirier, *Introduction to the Physics of the Earth's Interior* (Cambridge University Press, Cambridge, 1991).
[57]F. Occelli, D. L. Farber, J. Badro, C. M. Aracne, D. M. Teter, M. Hanfland, B. Canny, and B. Couzinet, Phys. Rev. Lett. **93**, 095502 (2004).